

Relativistic effects and deuteron photodisintegration with polarized and unpolarized gamma rays

L. N. Pandey and M. L. Rustgi

Physics Department, State University of New York at Buffalo, Buffalo, New York 14260

(Received 29 July 1985)

Angular distribution, asymmetry function, and polarization of the outgoing nucleons in deuteron photodisintegration are investigated employing the relativistic one-body charge density and two-body charge and current density effects with local and nonlocal contributions in pseudoscalar and pseudovector pion-nucleon couplings, and comparison is made with available experimental data. The angular distribution and polarization coefficients are reported for the super-soft core, Paris, Yale, and Hamada-Johnston potentials. The relativistic one-body and two-body corrections to the charge density increase the isotropic component of the angular distribution at lower energies but decrease it at higher energies. The changes in the polarization parameters are nearly the same for all the potentials, and all the potentials are found to reproduce the angular distribution, asymmetry function, and polarization of outgoing nucleons quite well at low and medium gamma ray energies.

I. INTRODUCTION

A theoretical investigation of deuteron photodisintegration can reveal important information about the radiative and nucleon-nucleon interaction in the deuteron. Within the framework of the traditional theory, the electric and magnetic multipoles contributions to the angular distribution, asymmetry function, and polarization of the outgoing nucleons in deuteron photodisintegration have been reported by a number of authors.¹⁻⁴ Because of the discrepancy between experimental and theoretical results, several workers⁵⁻¹⁵ have incorporated the two-body current and charge densities in the above-mentioned theory. All these calculations have been carried out within the nonrelativistic limit and only the local contributions of the two-body current and charge densities have been included. The inclusion of two-body current and charge densities improves¹⁴ the results but a noticeable discrepancy between the experimental data and theoretical values for polarization is still there even at very low energies.¹³

The contributions of the relativistic and retardation corrections to the dipole sum rules for a relativistic bound electron have been known for many years,¹⁶⁻¹⁸ but until recently they had not been included in nuclear photodisintegration calculations. Cambi, Mosconi, and Ricci¹⁹ have shown that the relativistic corrections to the one-body and two-body charge densities can help explain the well-known discrepancy between the theoretical and experimental values of the forward deuteron photodisintegration cross section.

Our aim in this paper is to include the relativistic corrections to one-body charge density and the two-body current and charge densities with its local and nonlocal contributions and study their effect on the angular distribution, asymmetry function, and polarization of the outgoing nucleons in deuteron photodisintegration for the

pseudoscalar (PS) and pseudovector (PV) pion-nucleon (πN) coupling for various available nucleon-nucleon potentials. A calculation parallel to that of Rustgi, Zernik, Breit, and Andrews (referred to as RZBA henceforth) is performed to incorporate the relativistic one-body and two-body charge densities with their local and nonlocal contributions. The same notation and conventions regarding geometry as used in RZBA are adopted here. The final state interaction between neutron and proton is taken into account, and transitions induced by electromagnetic multipoles $E1$, $M1$, and $E2$ are included. In Sec. II we will describe the interaction Hamiltonian for the relativistic one-body charge density and the two-body current and charge densities including both local and nonlocal contributions and the changes in the radial integrals of RZBA owing to these corrections. Section III is devoted to a discussion of our results and comparison with the available theoretical and experimental results.

II. CALCULATIONS

All the calculations presented below are performed by using the coordinate system shown in Fig. 1 of RZBA. The direction of the incoming photon is the positive z axis of a Cartesian coordinate system with its electric vector along the x axis. The z' axis of the second coordinate system with colatitude and azimuthal angles θ and ϕ , respectively, coincides with the direction of the outgoing proton. The direction cosines of the x' and y' axis are $(\cos\theta \cos\phi, \cos\theta \sin\phi, -\sin\theta)$ and $(-\sin\phi, \cos\phi, 0)$, respectively.

The interaction Hamiltonian given by Eq. (4) of RZBA, which includes the traditional $E1$, $E2$, and $M1$ electromagnetic multipoles on incorporating the relativistic one-body charge density effect and the two-body charge and current densities, can be written as

$$H' = -e \mathcal{E}_x \mathcal{A} \quad (1)$$

where,

$$\begin{aligned}
\mathcal{A} = & \frac{1}{2}(\mathbf{1}_E \cdot \mathbf{r}) + \frac{i}{8}(\mathbf{k} \cdot \mathbf{r})(\mathbf{1}_E \cdot \mathbf{r}) + \frac{f^2}{4M} \left\{ \frac{1}{3}(\phi_0 \sigma_1 \cdot \sigma_2 + \phi_2 S_{12}) \cdot \hat{\mathbf{r}} + (2\alpha_v \phi - \phi_1)[\sigma_1(\sigma_2 \cdot \hat{\mathbf{r}}) + \sigma_2(\sigma_1 \cdot \hat{\mathbf{r}})] \right\} \cdot \mathbf{1}_E \\
& + \frac{3}{2} \frac{f^2}{M} \phi \alpha_s [\sigma_1(\hat{\mathbf{r}} \cdot \sigma_2) - \sigma_2(\hat{\mathbf{r}} \cdot \sigma_1)] \cdot \mathbf{1}_E + \frac{f^2}{2M} \frac{1}{\mu} \{ \Phi_0 [(\sigma_2 \cdot \vec{\nabla})(\sigma_1 \cdot \hat{\mathbf{r}}) + (\sigma_1 \cdot \vec{\nabla})(\sigma_2 \cdot \hat{\mathbf{r}})] \hat{\mathbf{r}} + \frac{1}{3} [(3\Phi_1 + \Phi_2)\sigma_1 \cdot \sigma_2 + \Phi_2 S_{12}] \cdot \vec{\nabla} \} \cdot \mathbf{1}_E \\
& - \frac{1}{8M^2} \{(2\mu_v - 1)(\sigma_1 + \sigma_2) + 2(\mu_s + 1)(\sigma_1 - \sigma_2)\} \times \mathbf{P}_r \cdot \mathbf{1}_E \\
& + \frac{\hbar}{2Mc} [(\frac{1}{2}\mu_v + g_I + h_I)(\sigma_1 - \sigma_2) - \frac{1}{2}(\mu_s - \frac{1}{2})(\sigma_1 - \sigma_2) + (g_{II} + h_{II})T_{12}^{(-)}] \cdot \mathbf{1}_H , \tag{2}
\end{aligned}$$

S_{12} is usual tensor operator, M is the nucleon mass.

$$\mu_s = \mu_p + \mu_n, \quad \mu_v = \mu_p - \mu_n ,$$

$$\alpha_s(\text{PS}) = \frac{1}{2}\mu_s, \quad \alpha_s(\text{PV}) = \frac{1}{2},$$

$$\alpha_v(\text{PS}) = \frac{1}{2}(\mu_v + 1), \quad \alpha_v(\text{PV}) = \frac{1}{2},$$

μ_p and μ_n are the proton and neutron magnetic moments, respectively. In (2)

$$T_{12}^{(-)} = (\sigma_1 - \sigma_2) \cdot \hat{\mathbf{r}} \hat{\mathbf{r}} - \frac{1}{2}(\sigma_1 - \sigma_2) ,$$

$$\hat{\mathbf{r}} = \frac{\mathbf{r}}{|\mathbf{r}|} ,$$

and ϕ 's and Φ 's are defined in Refs. 20 and 21. The functions g_I , g_{II} , h_I , and h_{II} , are real scalar functions of $|\mathbf{r}| = |\mathbf{r}_1 - \mathbf{r}_2|$ and are given by Chemtob and Rho.²² The detailed forms of these for various meson exchange processes are described in Ref. 14.

The inclusion of the two-body current terms results¹³ in the following changes in the radial integrals M_S and M_D in Eqs. (18.1)–(18.3) of RZBA:

$$M_S \rightarrow M_S(\text{RZBA}) + 2M_S^0 - \frac{2\sqrt{2}}{3}M_D^0 , \tag{3}$$

$$M_D \rightarrow M_D(\text{RZBA}) + 2M_D^2 - \frac{2\sqrt{2}}{3}M_S^2 , \tag{4}$$

where

$$\begin{aligned}
I_0 \rightarrow & I_0(\text{RZBA}) + \gamma \int_0^\infty \left[U \left[\frac{f^2}{6M} e^{-\mu r} - \frac{2}{3} \frac{f^2}{M} Y_2(\mu r) - 6 \frac{f^2}{M} (\alpha_v - \frac{1}{2}) Y_1(\mu r) \right] - (1 - 2\mu_v) \frac{\mu}{M^2} U_1 \right. \\
& + 2 \frac{f^2}{M} \left\{ -(2\Phi_0 - \Phi_1 + \Phi_2) \frac{dU}{d(\mu r)} + \frac{1}{\mu r} (2\Phi_0 - \Phi_1 - \Phi_2) U - \frac{1}{2} \left[\frac{d}{d(\mu r)} (2\Phi_0 - \Phi_1 + \Phi_2) \right] U \right\} \\
& - \sqrt{2} W \left[\frac{f^2}{6M} e^{-\mu r} - \frac{2}{3} \frac{f^2}{M} Y_2(\mu r) \right] \\
& - (1 - 2\mu_v) \frac{\mu}{\sqrt{2}M^2} W_1 + 2\sqrt{2} \frac{f^2}{M} \left\{ (2\Phi_0 - \Phi_1 + \Phi_2) \frac{dW}{d(\mu r)} + \frac{1}{\mu r} (\Phi_0 - 2\Phi_1 + \Phi_2) W \right. \\
& \left. + \frac{1}{2} \left[\frac{d}{d(\mu r)} (2\Phi_0 - \Phi_1 + \Phi_2) \right] W \right\} \left. \right\} \mathcal{F}_0^1(kr) dr , \tag{7}
\end{aligned}$$

$$M_S^0 = \frac{\hbar}{Mc} \gamma \int_0^\infty U^1 \mathcal{F}_0(kr) (g_I + h_I) dr ,$$

$$M_S^2 = \frac{\hbar}{Mc} \gamma \int_0^\infty U^1 \mathcal{F}_2(kr) (g_{II} + h_{II}) dr ,$$

$$M_D^0 = \frac{\hbar}{Mc} \gamma \int_0^\infty W^1 \mathcal{F}_0(kr) (g_{II} + h_{II}) dr ,$$

$$M_D^2 = \frac{\hbar}{Mc} \gamma \int_0^\infty W^1 \mathcal{F}_2(kr) [(g_I + h_I) + \frac{1}{3}(g_{II} + h_{II})] dr .$$

The third term in Eq. (1) also leads to a modification of Eqs. (18.2) and (18.3) in RZBA, as it causes transitions to the 1P_1 state. This results in the addition of¹⁴

$$-6 \frac{f^2}{M} \cos \theta e^{iK_1} \alpha_s \int \left[U + \frac{W}{\sqrt{2}} \right] Y_1(\mu r)^1 \mathcal{F}_1(kr) dr \tag{5}$$

in Eq. (18.2), and

$$6 \frac{f^2}{M} \sin \theta \sin \phi e^{iK_1} \alpha_s \int \left[U + \frac{W}{\sqrt{2}} \right] Y_1(\mu r)^1 \mathcal{F}_1(kr) dr \tag{6}$$

in Eq. (18.3). Here

$$Y_1(x) = \frac{e^{-x}}{x^2} (1+x) .$$

The remaining charge density terms lead to the following modification of the $E1$ radial integrals:

$$\begin{aligned}
I_1 \rightarrow I_1(\text{RZBA}) + \gamma \int_0^\infty & \left[U \left[\frac{f^2}{6M} e^{-\mu r} + \frac{f^2}{3M} Y_2(\mu r) + \frac{4f^2}{M} (\alpha_v - \frac{1}{2}) Y_1(\mu r) \right] - (1-2\mu_v) \frac{\mu}{2M^2} U_1 \right. \\
& - 2 \frac{f^2}{M} \left\{ -(2\Phi_0 + \Phi_1 + \Phi_2) \frac{dU}{d(\mu r)} + \frac{1}{\mu r} (\Phi_0 + \Phi_1) U - \frac{1}{2} \left[\frac{d}{d(\mu r)} (2\Phi_0 + \Phi_1 + \Phi_2) \right] U \right\} \\
& + \frac{W}{\sqrt{2}} \left[\frac{f^2}{6M} e^{-\mu r} + \frac{f^2}{3M} Y_2(\mu r) - \frac{2f^2}{M} (\alpha_v - \frac{1}{2}) Y_1(\mu r) \right] (1-2\mu_v) \frac{\mu}{\sqrt{2}M^2} W_1 \\
& - \frac{2f^2}{M} \left\{ -\frac{1}{\sqrt{2}} (2\Phi_0 + \Phi_1 + \Phi_2) \frac{dW}{d(\mu r)} - \sqrt{2} \frac{1}{\mu r} (\Phi_0 + \Phi_1) W \right. \\
& \left. \left. - \frac{1}{2\sqrt{2}} \left[\frac{d}{d(\mu r)} (2\Phi_0 + \Phi_1 + \Phi_2) \right] W \right\} \right] \mathcal{F}_1^1(kr) dr , \tag{8}
\end{aligned}$$

$$\begin{aligned}
I_{\nu_r}^2 \rightarrow I_{\nu_r}^2(\text{RZBA}) + \gamma \int_0^\infty & \left[U \left[\frac{f^2}{6M} e^{-\mu r} - \frac{f^2}{15M} Y_2(\mu r) \right] + (1-2\nu_v) \frac{\mu}{2M^2} U_1 \right. \\
& + \frac{2}{5} \frac{f^2}{M} \left\{ (2\Phi_0 + 5\Phi_1 + \Phi_2) \frac{dU}{d(\mu r)} + \frac{1}{\mu r} (\Phi_0 - 5\Phi_1 - 2\Phi_2) + \frac{1}{2} \left[\frac{d}{d(\mu r)} (2\Phi_0 + 5\Phi_1 + \Phi_2) \right] U \right\} \\
& - \frac{W}{5\sqrt{2}} \left[\frac{f^2}{6M} e^{-\mu r} - \frac{11}{3} \frac{f^2}{M} Y_2(\mu r) - 30 \frac{f^2}{M} (\alpha_v - \frac{1}{2}) Y_1(\mu r) \right] - \frac{\sqrt{2}}{5} (1-2\mu_v) \frac{\mu}{M^2} W_1 \\
& + \frac{\sqrt{2}}{5} \frac{f^2}{M} \left\{ (14\Phi_0 - \Phi_1 + 7\Phi_2) \frac{dW}{d(\mu r)} \right. \\
& \left. \left. + \frac{2}{\mu r} (14\Phi_0 - \Phi_1 - 7\Phi_2) W + \frac{1}{2} \left[\frac{d}{d(\mu r)} (14\Phi_0 - \Phi_1 + 7\Phi_2) \right] W \right\} \right] \mathcal{U}_2^\tau dr , \tag{9}
\end{aligned}$$

and

$$\begin{aligned}
I_{\nu_r}^2 \rightarrow I_{\nu_r}^2(\text{RZBA}) + \gamma \int_0^\infty & \left[W \left[\frac{f^2}{6M} e^{-\mu r} - \frac{f^2}{3M} Y_2(\mu r) \right] - (1-2\mu_v) \frac{\mu}{2M^2} W_2 \right. \\
& + 2 \frac{f^2}{M} \left\{ -\frac{1}{3} (2\Phi_0 - 3\Phi_1 + \Phi_2) \frac{dW}{d(\mu r)} \right. \\
& \left. \left. + \frac{1}{3(\mu r)} (\Phi_0 - 9\Phi_1 + 2\Phi_2) W - \frac{1}{6} \left[\frac{d}{d(\mu r)} (2\Phi_0 - 3\Phi_1 + \Phi_2) \right] W \right\} + \sqrt{2} \frac{f^2}{3M} Y_2(\mu r) U \right. \\
& \left. + \frac{2\sqrt{2}}{3} \frac{f^2}{M} \left\{ +2(2\Phi_0 + \Phi_2) \frac{dU}{d(\mu r)} - 4 \frac{1}{\mu r} (2\Phi_0 + \Phi_2) U - \left[\frac{d}{d(\mu r)} (2\Phi_0 + \Phi_2) \right] U \right\} \right] \mathcal{V}_2^\tau dr , \tag{10}
\end{aligned}$$

where $\tau = (\alpha, \beta)$. U_1 , W_1 , and W_2 are defined as

$$U_1 = \frac{d}{d(\mu r)} U - \frac{U}{(\mu r)} , \tag{11a}$$

$$W_1 = \frac{dW}{d(\mu r)} + \frac{2W}{(\mu r)} , \tag{11b}$$

$$W_2 = \frac{dW}{d(\mu r)} - \frac{3W}{(\mu r)} , \tag{11c}$$

and

$$Y_2(x) = \frac{e^{-x}}{x} \left[1 + \frac{3}{x} + \frac{3}{x^2} \right] .$$

The contribution of relativistic correction for $S = T = 0$ is not included because its effect is expected to be negligible on the radial integrals.

The cross section and polarization of the outgoing nucleons can be calculated by substituting these modified radial integrals into Eqs. (9.5)–(9.8) of RZBA, which have been worked out for a combination of spin functions that transform like the components of a vector, both for the initial as well as final states and are written as

$$\sigma(\theta, \phi) = \mathcal{C}(k) \sum_{ij} |a_j|^2 |S_{ji}^\xi|^2 = \mathcal{C}(k) \bar{\sigma}, \quad (12)$$

$$P_x \bar{\sigma} = 2 \sum_i |a_i|^2 [\operatorname{Re}\{(S_{0i}^\xi)^* S_{1i}^\xi\} + \operatorname{Im}\{(S_{2i}^\xi)^* S_{3i}^\xi\}], \quad (13)$$

$$P_y \bar{\sigma} = 2 \sum_i |a_i|^2 [\operatorname{Re}\{(S_{0i}^\xi)^* S_{2i}^\xi\} + \operatorname{Im}\{(S_{3i}^\xi)^* S_{1i}^\xi\}], \quad (14)$$

$$P_z \bar{\sigma} = 2 \sum_i |a_i|^2 [\operatorname{Re}\{(S_{0i}^\xi)^* S_{3i}^\xi\} + \operatorname{Im}\{(S_{1i}^\xi)^* S_{2i}^\xi\}], \quad (15)$$

where

$$\mathcal{C}(k) = 2\omega e^2 / \hbar c v. \quad (16)$$

The cross section and polarization of the outgoing nu-

cleon for an unpolarized photon beam can be calculated by averaging the observables for the photon beam polarized along the x axis and the y axis.

The differential cross section and polarization of the outgoing nucleon with unpolarized gamma rays including all $E1$, $E2$, and $M1$ transitions may be expanded in powers of $\sin\theta$ and $\cos\theta$ and following RZBA, may be written as

$$\sigma(\theta) = a + b \sin^2\theta \pm c \cos\theta \pm d \cos\theta \sin^2\theta + e \sin^2\theta \cos^2\theta, \quad (17)$$

$$\sigma(\theta) P_x(\theta) = \sigma(\theta) P_z(\theta) = 0,$$

$$\sigma(\theta) P_y(\theta) = A \sin\theta + B \sin\theta \cos\theta$$

$$+ C \sin\theta \cos^2\theta + D \sin\theta \cos^3\theta. \quad (18)$$

The plus sign (minus sign) refers to proton (neutron). Knowing the cross section and polarization at various angles, these coefficients can be easily calculated.

III. RESULTS AND DISCUSSION

The above formalism has been used to calculate the angular distribution, asymmetry function, and polarization

TABLE I. Angular distribution parameters in $\mu\text{b}/\text{sr}$ for the super soft core potential B employing the two-body charge and current contributions to the conventional $E1$, $E2$, and $M1$ multipoles (I), and the relativistic correction in pseudoscalar (II) and pseudovector (III) pion-nucleon coupling.

E_γ (MeV)	Approximations	a	b	c	d	e
4.0	I	10.51	291.1	0.0222	25.20	0.545
	II	10.56	291.4	0.0222	25.20	0.545
	III	10.55	291.3	0.0216	25.20	0.545
10.0	I	4.612	157.9	0.2414	29.62	1.392
	II	4.694	159.2	0.2368	29.76	1.392
	III	4.628	159.1	0.2325	29.74	1.392
16.0	I	4.889	85.58	0.4494	21.80	1.392
	II	4.838	87.60	0.4311	22.06	1.392
	III	4.702	87.42	0.4214	22.04	1.392
20.0	I	5.147	61.39	0.5554	17.98	1.322
	II	4.971	63.70	0.5258	18.33	1.322
	III	4.792	63.51	0.5124	18.30	1.322
40.0	I					
	II	4.676	21.00	0.7134	8.796	0.9375
	III	4.357	20.87	0.6852	8.747	0.9375
50.0	I	5.242	11.66	0.8125	5.994	0.7895
	II	4.298	14.28	0.7183	6.585	0.7899
	III	3.942	14.19	0.6853	6.537	0.7899
100.0	I	3.883	2.810	0.7151	1.751	0.3762
	II	2.669	4.658	0.5860	2.273	0.3765
	III	2.280	4.726	0.5422	2.260	0.3765

TABLE II. Angular distribution parameters in $\mu\text{b}/\text{sr}$ for the super soft core potential D.

E_γ (MeV)	Approximations	a	b	c	d	e
4.0	I	11.89	298.0	0.270	25.92	0.5641
	II	11.93	298.3	0.0275	25.93	0.5641
	III	11.92	298.2	0.0268	25.93	0.5641
10.0	I	5.295	156.2	0.2887	29.61	1.407
	II	5.349	157.6	0.2827	29.76	1.407
	III	5.273	157.5	0.2778	29.74	1.407
16.0	I	5.564	82.68	0.5328	21.26	1.372
	II	5.460	84.69	0.5107	21.53	1.372
	III	5.304	84.69	0.4997	21.53	1.372
20.0	I	5.829	58.69	0.6576	17.35	1.288
	II	5.583	61.18	0.6225	17.72	1.288
	III	5.378	61.00	0.6072	17.69	1.288
40.0	I	6.061	17.12	0.9530	7.707	0.8849
	II	5.188	20.03	0.8583	8.326	0.8849
	III	4.821	20.01	0.8242	8.279	0.8849
50.0	I	5.832	10.95	0.9924	5.578	0.7415
	II	4.762	13.94	0.8766	6.249	0.7415
	III	4.353	13.87	0.8355	6.204	0.7415
100.0	I	4.390	2.846	0.9529	1.598	0.3561
	II	3.022	5.224	0.7510	1.959	0.3561
	III	2.559	5.317	0.7148	2.269	0.3561

TABLE III. Angular distribution parameters in $\mu\text{b}/\text{sr}$ for the Paris potential.

E_γ (MeV)	Approximations	a	b	c	d	e
4.0	I	11.15	282.1	0.0256	24.42	0.5286
	II	11.20	282.4	0.0249	24.42	0.5283
	III	11.20	282.4	0.0243	24.42	0.5283
10.0	I	5.250	152.5	0.2822	28.60	1.345
	II	5.381	154.1	0.2719	28.77	1.345
	III	5.381	154.1	0.2719	28.77	1.345
16.0	I	5.920	82.23	0.5269	20.96	1.340
	II	5.663	84.63	0.5047	21.28	1.340
	III	5.662	84.64	0.5046	21.28	1.340
20.0	I	5.920	58.83	0.6522	17.25	1.270
	II	5.699	61.37	0.6182	17.63	1.270
	III	5.510	61.14	0.6042	17.59	1.270
40.0	I					
	II	5.353	20.57	0.8549	8.482	0.8973
	III	5.014	20.39	0.8242	8.423	0.8973

TABLE III. (*Continued*).

E_γ (MeV)	Approximations	a	b	c	d	e
50.0	I	5.975	11.30	0.9756	5.733	0.7572
	II	4.930	14.27	0.8708	6.398	0.7576
	III	4.551	14.13	0.8346	6.339	0.7576
100.0	I	4.454	3.075	0.9005	1.735	0.3728
	II	3.134	5.284	0.7561	2.356	0.3732
	III	2.709	5.317	0.7036	2.331	0.3732

TABLE IV. Angular distribution parameters in $\mu\text{b}/\text{sr}$ for the Yale potential.

E_γ (MeV)	Approximations	a	b	c	d	e
4.0	I	11.30	281.5	0.0310	24.35	0.5270
	II	11.35	281.7	0.0219	24.36	0.5270
	III	11.34	281.7	0.0213	24.36	0.5270
10.0	I	5.147	152.3	0.2680	28.66	1.352
	II	5.229	153.6	0.2633	28.80	1.352
	III	5.162	153.4	0.2590	28.78	1.352
16.0	I	5.512	82.16	0.5105	20.99	1.345
	II	5.446	84.23	0.4925	21.27	1.345
	III	5.307	83.98	0.4828	21.23	1.345
20.0	I	5.822	58.89	0.6378	17.28	1.273
	II	5.617	61.27	0.6089	17.63	1.273
	III	5.435	61.00	0.5954	17.59	1.273
40.0	I					
	II	5.389	20.76	0.8808	8.494	0.8960
	III	5.057	20.51	0.8505	8.421	0.8660
50.0	I	6.041	11.62	1.013	5.766	0.7551
	II	5.004	14.48	0.9156	6.406	0.7550
	III	4.630	14.27	0.8787	6.331	0.7550
100.0	I	4.612	3.279	0.9981	1.711	0.3710
	II	3.260	5.518	0.8504	2.345	0.3710
	III	2.827	5.479	0.7914	2.296	0.3710

TABLE V. Angular distribution parameters in $\mu\text{b}/\text{sr}$ for the Hamada-Johnston potential.

E_γ (MeV)	Approximations	a	b	c	d	e
4.0	I	12.60	286.8	0.0262	25.42	0.5638
	II	12.64	287.4	0.0254	25.39	0.5612
	III	12.63	287.4	0.0247	25.39	0.5612
10.0	I	5.688	166.0	0.2971	30.87	1.440
	II	5.757	167.1	0.2919	30.96	1.437
	III	5.692	166.9	0.2875	30.94	1.437
16.0	I	5.841	92.06	0.5576	22.97	1.440
	II	5.774	94.30	0.5385	23.25	1.438
	III	5.639	94.04	0.5287	23.21	1.438

TABLE V. (*Continued*).

E_γ (MeV)	Approximations	a	b	c	d	e
20.0	I	6.094	66.80	0.6944	19.05	1.368
	II	5.900	69.37	0.6639	19.46	1.372
	III	5.723	69.09	0.6503	19.42	1.372
40.0	I					
	II	5.649	24.07	0.9566	9.543	0.9743
	III	5.322	23.81	0.9261	9.473	0.9743
50.0	I	6.307	13.63	1.099	6.570	0.8302
	II	5.278	16.78	0.9934	7.280	0.8348
	III	4.908	16.56	0.9564	7.206	0.8348
100.0	I	4.945	3.645	1.073	2.017	0.4200
	II	3.540	6.101	0.9952	2.715	0.4235
	III	3.108	6.054	0.8582	2.666	0.4235

TABLE VI. Polarizations parameters in $\mu\text{b}/\text{sr}$ for protons and neutrons for the super soft core potential B.

E_γ (MeV)	Approximations	A		B		C		D	
		Proton	Neutron	Proton	Neutron	Proton	Neutron	Proton	Neutron
4.0	I	-42.6	-43.0	-1.41	2.34	0.020	-0.020	0.000	0.000
	II	-42.2	-42.6	-1.39	2.35	0.021	-0.021	0.000	0.000
	III	-42.2	-42.6	-1.39	2.35	0.021	-0.021	0.000	0.000
10.0	I	-14.8	-15.3	1.81	4.52	0.275	-0.275	0.000	0.000
	II	-14.5	-15.0	1.88	4.59	0.287	-0.287	0.000	0.000
	III	-14.5	-15.0	1.85	4.56	0.285	-0.285	0.000	0.000
16.0	I	-8.16	-8.52	3.60	5.40	0.499	-0.499	-0.002	-0.002
	II	-7.90	-8.27	3.70	5.50	0.520	-0.520	-0.002	-0.002
	III	-7.87	-8.24	3.65	5.44	0.512	-0.512	-0.002	-0.002
20.0	I	-6.18	-6.49	4.11	5.52	0.596	-0.596	-0.004	-0.004
	II	-5.95	-6.26	4.23	5.63	0.620	-0.620	-0.004	-0.004
	III	-5.91	-6.23	4.16	5.57	0.609	-0.609	-0.004	-0.004
40.0	I								
	II	-2.70	-2.81	4.14	4.63	0.763	-0.763	-0.005	-0.005
	III	-2.64	-2.77	4.04	4.53	0.737	-0.737	-0.005	-0.005
50.0	I	-2.28	-2.31	3.39	3.71	0.706	-0.706	0.000	0.000
	II	-2.19	-2.24	3.69	4.01	0.752	-0.752	0.001	0.001
	III	-2.14	-2.19	3.58	3.90	0.721	-0.721	0.001	0.001
100.0	I	-1.32	-1.21	1.66	1.84	0.543	-0.543	0.043	0.034
	II	-1.32	-1.19	1.94	2.12	0.609	-0.609	0.035	0.035
	III	-1.24	-1.12	1.79	1.97	0.565	-0.565	0.035	0.035

TABLE VII. Polarizations parameters in $\mu\text{b}/\text{sr}$ for protons and neutrons for the super soft core potential D.

E_γ (MeV)	Approximations	A		B		C		D	
		Proton	Neutron	Proton	Neutron	Proton	Neutron	Proton	Neutron
4.0	I	-43.9	-44.3	-1.51	2.37	0.018	-0.018	0.000	0.000
	II	-43.5	-44.0	-1.49	2.38	0.019	-0.019	0.000	0.000
	III	-43.5	-44.0	-1.49	2.38	0.019	-0.19	0.000	0.00
10.0	I	-15.4	-16.1	1.50	4.35	0.256	-0.256	0.000	0.000
	II	-15.1	-15.8	1.57	4.21	0.269	-0.269	0.000	0.000
	III	-15.1	-15.7	1.54	4.39	0.265	-0.265	0.000	0.000
16.0	I	-8.51	-9.00	3.19	5.09	0.458	-0.458	-0.002	-0.002
	II	-8.24	-8.74	3.28	5.19	0.480	-0.480	-0.002	-0.002
	III	-8.20	-8.71	3.23	5.13	0.471	-0.471	-0.002	-0.002
20.0	I	-6.46	-6.88	3.66	5.16	0.543	-0.543	-0.004	-0.004
	II	-6.22	-6.64	3.78	5.28	0.568	-0.568	-0.004	-0.004
	III	-6.18	-6.60	3.71	5.21	0.556	-0.556	-0.004	-0.004
40.0	I								
	II	-2.83	-3.00	3.74	4.31	0.694	-0.694	-0.004	-0.004
	III	-2.78	-2.95	3.63	4.19	0.666	-0.666	-0.004	-0.004
50.0	I	-2.41	-2.48	3.07	3.46	0.647	-0.647	0.001	0.001
	II	-2.31	-2.39	3.37	3.76	0.690	-0.690	0.001	0.001
	III	-2.25	-2.34	3.25	3.64	0.656	-0.656	0.001	0.001
100.0	I	-1.44	-1.34	1.61	1.83	0.541	-0.541	0.031	0.031
	II	-1.45	-1.33	1.97	2.19	0.608	-0.608	0.031	0.031
	III	-1.36	-1.25	1.81	2.03	0.559	-0.559	0.031	0.031

TABLE VIII. Polarizations parameters in $\mu\text{b}/\text{sr}$ for protons and neutrons for the Paris potential.

E_γ (MeV)	Approximations	A		B		C		D	
		Proton	Neutron	Proton	Neutron	Proton	Neutron	Proton	Neutron
4.0	I	-42.2	-42.7	-1.34	2.38	0.022	-0.022	0.000	0.000
	II	-41.87	-42.4	-1.33	2.39	0.023	-0.023	0.000	0.000
	III	-41.86	-42.4	-1.33	2.39	0.023	-0.023	0.000	0.000
10.0	I	-15.3	-15.9	2.04	4.83	0.296	-0.296	0.000	0.000
	II	-15.0	-15.6	2.13	4.92	0.316	-0.316	0.000	0.000
	III	-15.0	-15.6	2.13	4.92	0.316	-0.316	0.000	0.000
16.0	I	-8.62	-9.10	3.84	5.73	0.533	-0.533	-0.002	-0.002
	II	-8.38	-8.86	3.99	5.88	0.562	-0.562	-0.002	-0.002
	III	-8.38	-8.86	3.99	5.88	0.562	-0.562	-0.002	-0.002
20.0	I	-6.62	-7.02	4.31	5.81	0.628	-0.628	-0.002	-0.002
	II	-6.37	-6.78	4.46	5.93	0.657	-0.657	-0.004	-0.004
	III	-6.33	-6.75	4.39	5.89	0.646	-0.646	-0.004	-0.004
40.0	I								
	II	-3.02	-3.17	4.29	4.85	0.788	-0.788	-0.004	-0.004
	III	-2.96	-3.12	4.18	4.73	0.762	-0.762	-0.004	-0.004
50.0	I	-2.57	-2.62	3.48	3.85	0.715	-0.715	0.001	0.001
	II	-2.48	-2.55	3.86	4.22	0.779	-0.779	0.001	0.001
	III	-2.42	-2.49	3.73	4.10	0.747	-0.747	0.001	0.001
100.0	I	-1.51	-1.38	1.82	2.02	0.582	-0.582	0.038	0.038
	II	-1.54	-1.38	2.20	2.40	0.676	-0.676	0.038	0.038
	III	-1.45	-1.30	2.02	2.22	0.627	-0.672	0.038	0.038

TABLE IX. Polarizations parameters in $\mu\text{b}/\text{sr}$ for protons and neutrons for the Yale potential.

E_γ (MeV)	Approximations	A		B		C		D	
		Proton	Neutron	Proton	Neutron	Proton	Neutron	Proton	Neutron
4.0	I	-42.0	-43.0	-1.35	2.38	0.022	-0.022	0.000	0.000
	II	-42.0	-42.6	-1.33	2.39	0.023	-0.023	0.000	0.00
	III	-42.0	-42.6	-1.34	2.39	0.022	-0.022	0.000	0.000
10.0	I	-15.2	-16.0	2.06	4.86	0.305	-0.305	0.000	0.000
	II	-14.9	-15.7	2.14	4.94	0.317	-0.317	0.000	0.00
	III	-14.9	-15.7	2.11	4.91	0.314	-0.314	0.000	0.000
16.0	I	-8.60	-9.23	3.89	5.80	0.549	-0.549	-0.001	-0.001
	II	-8.33	-8.96	4.00	5.91	0.569	-0.569	-0.001	-0.001
	III	-8.30	-8.93	3.94	5.85	0.561	-0.561	-0.001	-0.001
20.0	I	-6.63	-7.16	4.36	5.88	0.650	-0.650	-0.002	-0.002
	II	-6.38	-6.92	4.50	6.02	0.672	-0.672	-0.002	-0.002
	III	-6.34	-6.88	4.43	5.95	0.661	-0.661	-0.002	-0.002
40.0	I	-3.06	-3.31	4.30	4.90	0.806	-0.806	-0.001	-0.001
	II	-3.00	-3.25	4.18	4.78	0.781	-0.781	-0.001	-0.001
	III	-3.00	-3.25	4.18	4.78	0.781	-0.781	-0.001	-0.001
50.0	I	-2.63	-2.77	3.51	3.92	0.745	-0.745	0.005	0.005
	II	-2.52	-2.67	3.86	4.27	0.792	-0.792	0.005	0.005
	III	-2.45	-2.61	3.72	4.13	0.762	-0.762	0.005	0.005
100.0	I	-1.56	-1.49	1.84	2.04	0.586	-0.586	0.034	0.034
	II	-1.55	-1.46	2.19	2.40	0.663	-0.663	0.034	0.034
	III	-1.45	-1.37	2.00	2.21	0.615	-0.615	0.034	0.034

TABLE X. Polarizations parameters in $\mu\text{b}/\text{sr}$ for protons and neutrons for the Hamada-Johnston potential.

E_γ (MeV)	Approximations	A		B		C		D	
		Proton	Neutron	Proton	Neutron	Proton	Neutron	Proton	Neutron
4.0	I	-43.7	-44.3	-1.56	2.36	0.017	-0.017	0.000	0.000
	II	-43.4	-44.0	-1.56	2.37	0.018	-0.018	0.000	0.000
	III	-43.4	-44.0	-1.56	2.37	0.018	-0.018	0.000	0.00
10.0	I	-16.8	-17.6	1.42	4.50	0.259	-0.259	0.000	0.000
	II	-16.5	-17.3	1.48	4.57	0.269	-0.269	0.000	0.000
	III	-16.5	-17.3	1.46	4.54	0.267	-0.267	0.000	0.000
16.0	I	-9.54	-10.2	3.28	5.41	0.479	-0.479	-0.002	-0.002
	II	-9.25	-9.90	3.38	5.51	0.497	-0.497	-0.002	-0.002
	III	-9.21	-9.86	3.33	5.46	0.490	-0.490	-0.002	-0.002
20.0	I	-7.29	-7.84	3.87	5.57	0.578	-0.578	-0.003	-0.003
	II	-7.03	-7.58	3.99	5.69	0.601	-0.601	-0.003	-0.003
	III	-6.99	-7.54	3.93	5.63	0.591	-0.591	-0.003	-0.003
40.0	I	-3.23	-3.47	4.26	4.94	0.793	-0.793	-0.002	-0.002
	II	-3.18	-3.42	4.16	4.83	0.769	-0.769	-0.002	-0.002
	III	-3.18	-3.42	4.16	4.83	0.769	-0.769	-0.002	-0.002
50.0	I	-2.75	-2.86	3.59	4.07	0.752	-0.752	0.004	0.004
	II	-2.63	-2.76	3.93	4.41	0.811	-0.811	0.004	0.004
	III	-2.57	-2.71	3.80	4.28	0.782	-0.782	0.004	0.004
100.0	I	-1.62	-1.50	2.00	2.27	0.648	-0.648	0.042	0.042
	II	-1.63	-1.49	2.37	2.63	0.746	-0.746	0.042	0.042
	III	-1.54	-1.41	2.18	2.45	0.696	-0.696	0.042	0.042

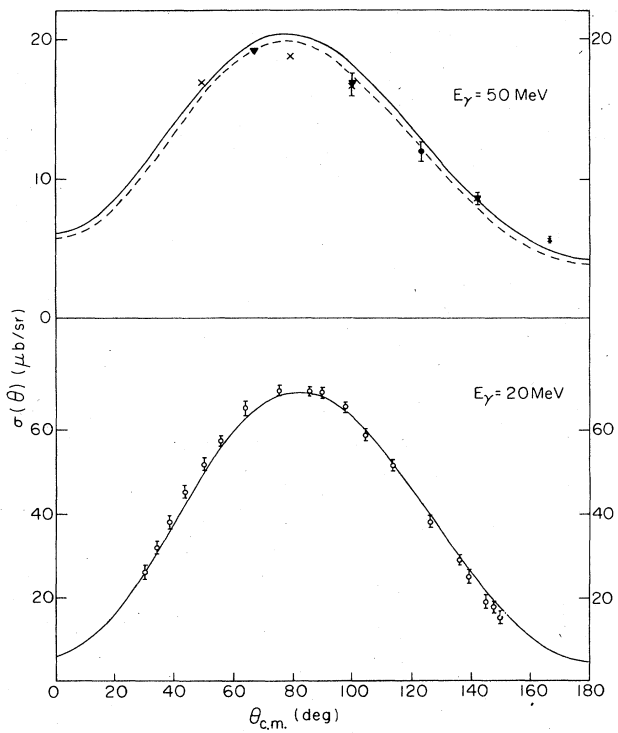


FIG. 1. Differential cross section for deuteron photodisintegration in approximation II (solid line) and approximation III (dotted line) at $E_\gamma = 20$ and 50 MeV for the Paris potential. The experimental results of the various investigators are as follows: solid circles and inverted triangles for those of Weissman (Ref. 28), crosses for those of Galey (Ref. 29), and open circles for those of Skopik *et al.* (Ref. 30).

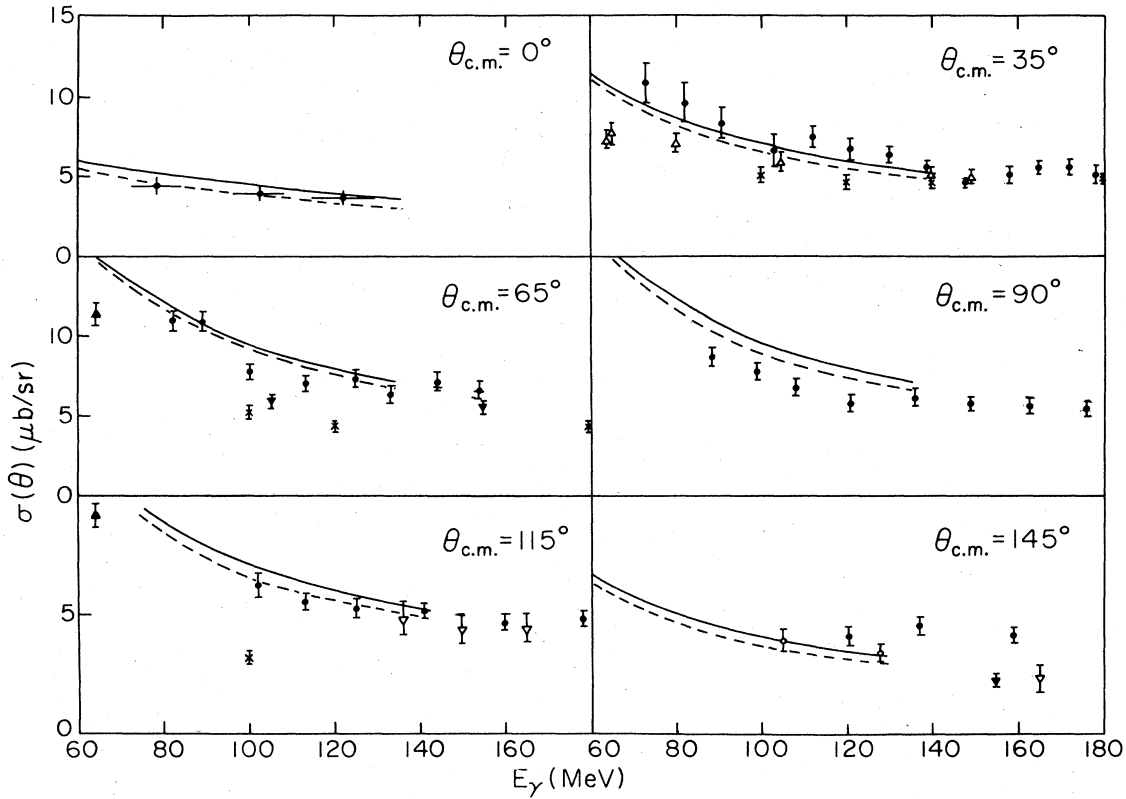


FIG. 2. Differential cross section for deuteron photodisintegration in approximation II (solid line) and approximation III (dotted line) for the Hamada-Johnston potential at $\theta_{\text{c.m.}} = 0^\circ, 35^\circ, 65^\circ, 90^\circ, 115^\circ$, and 145° . The experimental results for $\theta_{\text{c.m.}} = 0^\circ$ are those of Hughes *et al.* (Ref. 31). The experimental data of various investigators at other angles are as follows: solid circles for those of Dougan *et al.* (Ref. 32); solid inverted triangles for those of Allen (Ref. 33); open inverted triangles for those of Whalin *et al.* (Ref. 34); crosses for those of Kose *et al.* (Ref. 35); solid inverted triangles for those of Keck and Tollestrup (Ref. 36); open inverted triangles for those of Dixon *et al.* (Ref. 37).

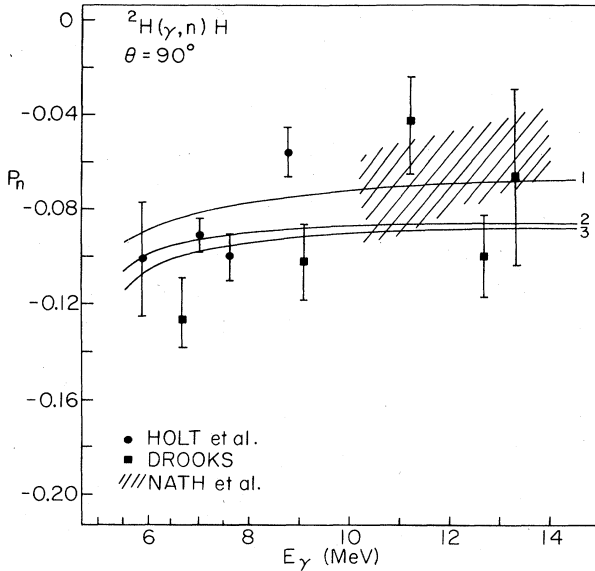


FIG. 3. Comparison of the present work for polarization result with the data of Holt *et al.* (Ref. 41), Nath *et al.* (Ref. 42), and Drook (Ref. 43). Curve 1 is the result of the investigation of Ref. 14 for the potential SSC-B excluding the two-body charge and current effects, curve 2 results when the two-body charge and current effects are included, and curve 3 includes the relativistic effect also.

of the outgoing nucleons in deuteron photodisintegration for the Paris,²³ Yale,²⁴ Hamad-Johnston²⁵ (HJ), Hamada-Johnston modified (HJM), and the various super soft core^{26,27} (SSC-A, SSC-B, SSC-C, SSC-D) nucleon-nucleon potentials at various photon energies taking relativistic corrections, two-body current, and charge densities with their local and nonlocal contributions. The super soft core potential of Ref. 27 is referred to as SSC-D here. The calculations are performed in three steps. In approximation I, the results of Rustgi, Vyas, and Rustgi,¹⁴ which include the local contribution of the two-body current and charge densities without relativistic correction, are report-

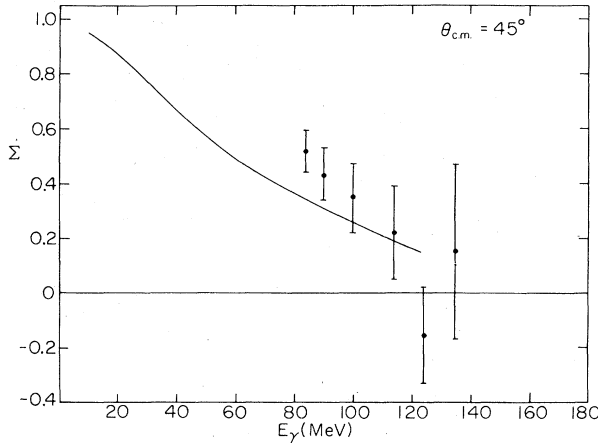


FIG. 4. The asymmetry function $\Sigma(\theta)$ for the SSC-B potential at $\theta_{c.m.} = 45^\circ$. The experimental points are those of Liu (Ref. 45).

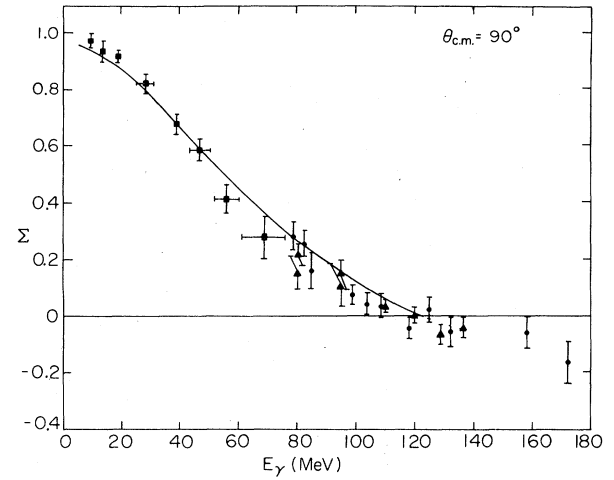


FIG. 5. The asymmetry function $\Sigma(\theta)$ for the SSC-B potential at $\theta_{c.m.} = 90^\circ$. The experimental points are those of Liu (Ref. 45) and Bianco *et al.* (Refs. 46 and 47).

ed. The results on the inclusion of local and nonlocal contributions of the two-body current and charge densities with relativistic corrections is pseudoscalar (PS) and pseudovector (PV) pion-nucleon (πN) coupling are listed in approximation II and III, respectively.

The cross section parameters—a, b, c, d, and e—for the SSC-B, SSC-D, Paris, Yale, and Hamada-Johnston potentials at photon energies $E_\gamma = 4, 10, 16, 20, 40, 50$, and 100 MeV are given in Tables I–V. Owing to the similarity amongst the angular distribution and polarization coefficients for the SSC-A, SSC-B, and SSC-C potentials and those between the coefficients for the Yale and HJM potentials, we have chosen to report the coefficients for the SSC-B and Yale potentials only. It is clear from these tables that the relativistic effect in PS πN coupling case increases parameter a a little bit at lower photon energies and decreases it by a substantial amount at higher energies, whereas parameter b is increased for all energies although at lower energies the increase is not as significant

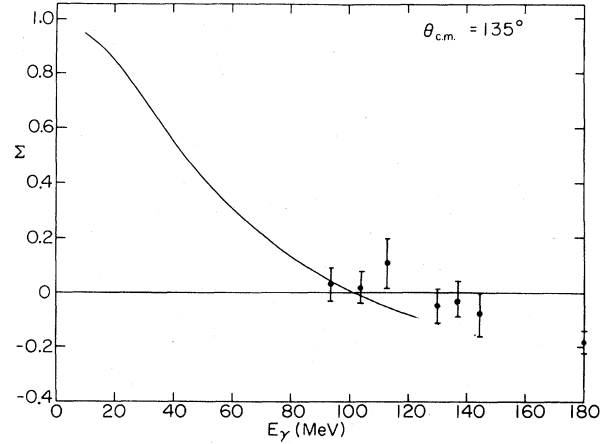


FIG. 6. The asymmetry function $\Sigma(\theta)$ for the SSC-B potential at $\theta_{c.m.} = 135^\circ$. The experimental points are those of Liu (Ref. 45).

as at higher energies. The values of a and b parameters in PV πN coupling are found to be a little lower than the values for the PS πN coupling except at 100 MeV where for the case of PV πN coupling the value of b is higher than that for the PS πN coupling case. The differences in the parameters for PS and PV πN coupling cases are small at lower energies. Parameters c and d are decreased and increased, respectively, for both the πN couplings due to the relativistic correction. The values of parameters c and d for the PV πN coupling are found to be smaller than the value for the PS πN coupling case. Parameter e remains practically unchanged. The changes in parameters a , b , c , and d will not only shift the angular distribution curve but will also change its shape.

The polarization parameters A, B, C, and D of the outgoing proton and neutron for the SSC-B, SSC-D, Paris, Yale, and Hamada-Johnston potential at photon energies $E_\gamma = 4, 10, 16, 20, 40$, and 100 MeV are listed in Tables VI-X. Owing to the relativistic correction, for both proton and neutron, parameter A is decreased, parameters B and C are increased but parameter D is unchanged. Although there are some changes in the values of these coefficients for different potentials, these changes are too small to enable us to draw any conclusion from them.

A comparison with the experimental data for the angular distribution, asymmetry function, and the polarization of the outgoing nucleons in deuteron photodisintegration is made in Figs. 1 and 2, Fig. 3, and Figs. 4-6, respectively. In Fig. 1, we have plotted the cross section versus angles of outgoing proton at photon energies $E_\gamma = 20$ and 50 MeV for the Paris potential and compared them with the experimental data of Weissman and Schultz,²⁸ Galey,²⁹ and Skopik *et al.*³⁰ It is clear from Fig. 1 that it is not possible to distinguish between the PS and PV πN coupling results at 20 MeV. The PV values are smaller than those for PS coupling at 50 MeV but both fit the experimental data quite well at both energies. Figure 2 shows the differential cross sections for protons in PS and PV πN coupling for the Hamada-Johnston potential at angles

$\theta_{c.m.} = 0^\circ, 35^\circ, 65^\circ, 90^\circ, 115^\circ$, and 145° and the results with the relativistic correction reproduce the experimental data at all angles very well. We have also compared the differential cross section data of Fuller,³⁸ Bosch *et al.*,³⁹ and Halpern and Weinstock⁴⁰ with our calculations and found that with a suitable normalization factor which is smaller than that of approximation I, the fit to the experimental data is excellent.

In Fig. 3, the results for the potential SSC-B without the two-body effect, with the two-body effects, and two-body effects including relativistic corrections are labeled as 1, 2, and 3, respectively. It is clear that the result when two-body effects are excluded gives good agreement with the data of Holt *et al.*⁴¹ and others,^{42,43} but in view of the large uncertainties in the data, curves 2 and 3, which have two-body effects and two-body effects including relativistic correction, respectively, also fit equally well. However, as has been pointed out in Ref. 13, the two-body contributions decrease the polarization but the relativistic corrections lower the curve even further. There is no change found in the comparison with the experimental data of Jewell *et al.*⁴⁴ (not shown) at $E_\gamma = 2.75$ MeV which is also clear from Tables VI-X where no changes are found in the polarization parameters at lower energies.

In Figs. 4-6, we have shown the variation of asymmetry functions $\Sigma(\theta)$ with photon energies at $\theta_{c.m.} = 45^\circ, 90^\circ$, and 135° and found that the relativistic effects make the curve fit the experimental data quite well at higher energies without affecting the agreement at lower energies.

In conclusion, we find that the relativistic effects reproduce the experimental data quite well at all energies considered here. Both the pseudoscalar and pseudovector πN couplings yield almost identical fits to the experimental data.

This work was partially supported by the National Aeronautics and Space Administration under Grant No. NAG1442.

-
- ¹M. L. Rustgi, W. Zernik, G. Breit, and D. J. Andrews, Phys. Rev. **120**, 1181 (1960).
²F. Partovi, Ann. Phys. (N.Y.) **27**, 79 (1964).
³M. L. Rustgi, T. S. Sandhu, and O. P. Rustgi, Phys. Rev. C **20**, 24 (1979).
⁴R. Vyas, M. Chopra, and M. L. Rustgi, Phys. Rev. C **25**, 1801 (1982).
⁵D. O. Riska and G. E. Brown, Phys. Lett. **38B**, 193 (1972).
⁶H. Hyuga, A. Arima, and K. Shimizu, Nucl. Phys. **A336**, 363 (1980).
⁷E. Hadjimichael, Phys. Rev. Lett. **31**, 183 (1973).
⁸J. Hockert, D. O. Riska, M. Gari, and A. Huffman, Nucl. Phys. **A217**, 14 (1973).
⁹S. Rab and D. S. Koltun, Phys. Rev. C **26**, 658 (1982).
¹⁰A. Cambi, B. Masconi, and P. Ricci, Phys. Rev. C **23**, 992 (1981); Reeta Vyas and M. L. Rustgi, *ibid.* **26**, 1399 (1982).
¹¹E. Hadjimichael, Phys. Lett. **46B**, 147 (1973).
¹²H. Arenhovel, W. Fabian, and H. G. Miller, Phys. Lett. **52B**, 303 (1974).
¹³M. L. Rustgi, R. Vyas, and M. Chopra, Phys. Rev. Lett. **50**, 236 (1982); M. L. Rustgi and R. Vyas, Phys. Lett. **121B**, 365 (1983).
¹⁴M. L. Rustgi, Reeta Vyas, and O. P. Rustgi, Phys. Rev. C **29**, 785 (1984).
¹⁵M. L. Rustgi, R. D. Nunemaker, and R. Vyas, Can. J. Phys. **62**, 1064 (1984).
¹⁶J. S. Levinger, M. L. Rustgi, and K. Okamoto, Phys. Rev. **106**, 1191 (1957).
¹⁷J. L. Friar and S. Fallieros, Phys. Rev. C **11**, 1191 (1975).
¹⁸K. M. Schmitt and H. Arenhovel, Z. Phys. A **320**, 311 (1985).
¹⁹A. Cambi, B. Mosconi, and P. Ricci, Phys. Rev. Lett. **48**, 462 (1982).
²⁰A. Cambi, B. Mosconi, and P. Ricci, Universita Degli Studi Di Firenze, Italy, report 148-84, 1984.
²¹L. N. Pandey and M. L. Rustgi, Phys. Rev. C (in press).
²²M. Chemtob and M. Rho, Nucl. Phys. **A163**, 1 (1971).
²³M. Lacombe, B. Loriseau, J. M. Richard, R. Vinh Mau, J. Cote, P. Pires, and R. de Tourreil, Phys. Rev. C **21**, 861 (1980).
²⁴K. E. Lassila, M. H. Hull, Jr., H. M. Ruppel, F. A. McDonald, and G. Breit, Phys. Rev. **126**, 881 (1962).
²⁵T. Hamada and I. D. Johnston, Nucl. Phys. **34**, 382 (1962).
²⁶R. de Tourreil and D. W. L. Sprung, Nucl. Phys. **A201**, 593 (1973).

- ²⁷R. de Tourreil, B. Rouben, and D. W. L. Sprung, Nucl. Phys. **A242**, 445 (1975).
- ²⁸B. Weissmann and H. L. Schultz, Nucl. Phys. **A174**, 129 (1971).
- ²⁹J. A. Galey, Phys. Rev. **117**, 763 (1960).
- ³⁰D. M. Skopik, Y. M. Shin, M. C. Phenneger, and J. J. Murphy II, Phys. Rev. C **9**, 531 (1974).
- ³¹R. J. Hughes, A. Zieger, H. Waffler, and B. Ziegler, Nucl. Phys. **A267**, 329 (1976).
- ³²P. Dougan, V. Ramsay, and W. Stiefler, Z. Phys. A **280**, 341 (1977).
- ³³L. Allen, Jr., Phys. Rev. **98**, 705 (1955).
- ³⁴B. A. Whalin, B. D. Schriever, and A. O. Hanson, Phys. Rev. **101**, 377 (1956).
- ³⁵R. Kose, W. Paul, K. Stockhorst, and K. H. Kissler, Z. Phys. **202**, 364 (1967).
- ³⁶J. C. Keck and A. V. Tollestrup, Phys. Rev. **101**, 360 (1956).
- ³⁷D. R. Dixon and K. C. Bandtel, Phys. Rev. **104**, 1730 (1956).
- ³⁸E. G. Fuller, Phys. Rev. **79**, 303 (1950).
- ³⁹R. Bosch, J. Lang, R. Muller, and W. Wolfle, Helv. Phys. Acta **36**, 657 (1963).
- ⁴⁰J. Halpern and E. V. Weinstock, Phys. Rev. **90**, 934 (1953).
- ⁴¹R. J. Holt, K. Stephenson, and J. R. Specht, Phys. Rev. Lett. **50**, 577 (1983).
- ⁴²R. Nath, F. W. K. Firk, and H. L. Schultz, Nucl. Phys. **A194**, 49 (1972).
- ⁴³L. J. Drook, Ph.D. thesis, Yale University, 1976.
- ⁴⁴R. W. Jewell, W. John, J. E. Sherwood, and D. H. White, Phys. Rev. **139**, B71 (1965).
- ⁴⁵F. F. Liu, Phys. Rev. **138**, B1443 (1965).
- ⁴⁶W. Del Bianco, H. Jeremie, M. Irshad, and G. Kajrys, Nucl. Phys. **A343**, 121 (1980).
- ⁴⁷W. Del Bianco, L. Federici, G. Giordano, G. Matone, G. Pasquariello, P. Picozza, R. Caboi, L. Casano, M. D. De Pascale, L. Ingrosso, M. Mattioli, E. Poldi, C. Sshaerf, P. Pelfer, D. Prosperi, S. Frullani, B. Giorlami, and H. Jermie, Phys. Rev. Lett. **47**, 1118 (1981).